

Mean-Square Electric Dipole Moment of Oligo- and Poly(dimethylsiloxane)s in Dilute Solutions

Takeshi Yamada, Takenao Yoshizaki, and Hiromi Yamakawa*

Department of Polymer Chemistry, Kyoto University, Kyoto 606-01, Japan

Received October 3, 1991; Revised Manuscript Received November 18, 1991

ABSTRACT: The mean-square electric dipole moment $\langle \mu^2 \rangle$ was determined for 18 well-fractionated samples of oligo- and poly(dimethylsiloxane)s (PDMS) with the weight-average molecular weights ranging from 1.62×10^2 (monomer) to 1.83×10^6 in cyclohexane at 25.0 °C. Although cyclohexane is not a Θ solvent for PDMS, it is concluded from the results that the excluded-volume effect on $\langle \mu^2 \rangle$ of PDMS having type-B dipoles may be regarded as negligibly small if any. The ratio $\langle \mu^2 \rangle / x_w$ as a function of the weight-average degree of polymerization x_w exhibits a maximum as in the case of literature data for undiluted PDMS. It is shown that the helical wormlike (HW) chain theory may well explain the data with the three sets of values of the HW model parameters, $\lambda^{-1}\kappa_0 = 2.6$, $\lambda^{-1}\tau_0 = 0$, and $\lambda^{-1}M_L = 450$, along with the value 0.29 D of the permanent electric dipole moment per repeat unit, where κ_0 and τ_0 are the constant curvature and torsion, respectively, of its characteristic helix taken at the minimum of energy, λ^{-1} is the static stiffness parameter, and M_L is the shift factor as defined as the molecular weight per unit contour length. The two parameters λ^{-1} and M_L cannot be determined separately from the data for $\langle \mu^2 \rangle$ alone, since it is not related to the chain dimension. The value 2.6 of $\lambda^{-1}\kappa_0$ coincides with the one determined in a previous analysis of the literature data for $\langle \mu^2 \rangle$ for undiluted PDMS. The maximum in $\langle \mu^2 \rangle / x_w$ and also the values of $\lambda^{-1}\kappa_0$ and $\lambda^{-1}\tau_0$ indicate that the PDMS chain has rather strong helical nature, as expected from its chemical structure.

Introduction

In a series of recent systematic experimental studies of dilute solutions of oligomers and polymers in the unperturbed (Θ) state, we have been analyzing the data obtained for equilibrium conformational and steady-state transport properties on the basis of the helical wormlike (HW) chain model.^{1,2} The polymers investigated so far are atactic polystyrene (a-PS)³⁻⁶ and atactic poly(methyl methacrylate) (a-PMMA)^{7,8} as asymmetric polymers and polyisobutylene (PIB)⁹ as a symmetric one. It has been found that among these, the a-PMMA chain is of strong helical nature and thus a typical example of the HW chain, while the PIB chain may well be mimicked by the Kratky-Porod (KP) wormlike chain model¹⁰ as a special case of the former. In the present and forthcoming papers, we proceed to make a similar study of poly(dimethylsiloxane) (PDMS), which is a symmetric polymer but may be expected to exhibit rather strong helical nature.

The backbone of the PDMS chain is composed of alternating bonded silicon (Si) and oxygen (O) atoms and the bond angles at the Si and O atoms are appreciably different from each other. Therefore, its chain contour takes a circular shape instead of a straight line in the all-trans conformation, so that the situation is similar to that in the case of the a-PMMA chain. This leads us to the anticipation that the PDMS chain is another typical example of the HW chain. Indeed, this has already been confirmed from a preliminary analysis of literature data^{11,12} for the mean-square electric dipole moment $\langle \mu^2 \rangle$ for undiluted PDMS on the basis of the HW model.¹³ For our purposes, especially for a determination of the HW model parameters, however, it is desirable to obtain dilute-solution data in the unperturbed state.

In the case of the typical HW chain, its model parameters may be determined from the mean-square radius of gyration $\langle S^2 \rangle$ or the intrinsic viscosity $[\eta]$, as done for a-PMMA.^{7,8} We must then determine $\langle S^2 \rangle$ from small-angle X-ray scattering and light scattering measurements as far as our facilities readily available are utilized. However, our preliminary measurements showed that it was impossible since irradiation with X-ray caused de-

naturation, probably gelation, of a PDMS sample. On the other hand, the determination of all the model parameters from data for $[\eta]$ alone was also impossible since its behavior looked like that for the KP chain.¹⁴ This is due to the very small hydrodynamic thickness of the PDMS chain.¹⁴ Thus we have decided to start the study of PDMS from a determination of some of the HW model parameters from its $\langle \mu^2 \rangle$ in dilute solution. Its possibility may be expected from the previous analysis.

There is no difficulty in an application of the HW theory of $\langle \mu^2 \rangle$ to PDMS. The reasons for this are that, as is well-known, its chain has type-B dipoles¹⁵ perpendicular to the chain contour and that this local dipole moment vector may be attached unambiguously in a localized Cartesian coordinate system affixed to the HW chain, as discussed previously.¹³ However, there arises an experimental problem. For the determination of $\langle \mu^2 \rangle$ in dilute solution, we must use a completely or nearly nonpolar solvent. Thus we chose cyclohexane as a solvent. This choice may not meet the present purpose since it is not a Θ solvent for PDMS. However, in anticipation of the analysis of the results, we note that the excluded-volume effect on $\langle \mu^2 \rangle$ of PDMS having type-B dipoles may be regarded as negligibly small if any.

Experimental Section

Materials. All the PDMS samples used in this work are fractions from the commercial samples supplied from Toshiba Silicon Co., Ltd., named Low Boil Fractions, 5CS, TSF451-10, TSF451-100, TSF451-500, and TSF451-50M. Both ends of the PDMS chain in these original samples are terminated by methyl groups, and the chemical formula of the x -mer with x the degree of polymerization is given by



Test samples of the monomer through the heptamer were separated from the original sample Low Boil Fraction by fractional distillation under reduced pressure, i.e., at 85.5 mmHg at 41 °C for $x = 1$, at 21.0 mmHg at 52 °C for $x = 2$, at 11.0 mmHg at 45 °C for $x = 3$, at 4.5 mmHg at 74 °C for $x = 4$, at 2.0 mmHg at 94 °C for $x = 5$, at 2.0 mmHg at 118 °C for $x = 6$, and at 2.0 mmHg at 135 °C for $x = 7$. Then the mixture of the residue of the distillation and the original samples 5CS and TSF451-10 was

Table I
Values of M_w , x_w , and M_w/M_n for Oligo- and Poly(dimethylsiloxane)s

sample	M_w	x_w	M_w/M_n
ODMS1	1.62×10^2	1	1.00
ODMS2	2.37×10^2	2	1.00
ODMS3	3.11×10^2	3	1.00
ODMS4	3.85×10^2	4	1.00
ODMS5	4.59×10^2	5	1.00
ODMS6	5.33×10^2	6	1.00
ODMS7	6.08×10^2	7	1.00
ODMS10	8.15×10^2	9.8	1.00
ODMS11	9.24×10^2	11.3	1.01
ODMS14	1.14×10^3	14.2	1.01
ODMS18	1.39×10^3	17.5	1.01
ODMS24	1.90×10^3	24.4	1.01
ODMS35	2.67×10^3	34.8	1.02
ODMS71	5.37×10^3	71.2	1.06
PDMS1	8.26×10^3	110	1.05
PDMS2	2.21×10^4	297	1.08
PDMS3	3.19×10^4	429	1.08
PDMS20	1.83×10^5	2470	1.05

separated into fractions of narrow molecular weight distribution by preparative gel permeation chromatography (GPC) with two serially connected Tosoh G2000H₈ (600 × 50 mm) columns using chloroform as an eluent. Test samples with higher molecular weights were separated by fractional precipitation from the original sample TSF451-100 using methyl ethyl ketone as a solvent and methanol as a precipitant and from the original samples TSF451-500 and TSF451-50M using ethyl acetate as a solvent and methanol as a precipitant. The precipitation was repeated several times to obtain test samples of sufficiently narrow molecular weight distribution. The solvents and nonsolvent were first evacuated from the main fractions thus obtained by preparative GPC and by fractionation. Then they were dried under reduced pressure at 25–50 °C from their cyclohexane solutions after filtration through a Teflon membrane of pore size 0.45 μm except for the highest molecular weight sample. The latter was freeze-dried from its cyclohexane solution after filtration through a membrane of the same kind.

The first and second fractions from the fractional distillation were identified with the monomer and dimer, respectively, by ¹H NMR spectroscopy. The spectra for these fractions were recorded on a JEOL JNM-FX-90Q spectrometer at 89.6 MHz in chloroform-*d* containing cyclohexane as an internal standard at 30 °C. The measurements were carried out with a radio-frequency pulse angle of 90° and a pulse repetition time of 30 s. For the present purpose, we have only to know the number of kinds of proton (i.e., only one kind for $x = 1$ and two kinds for $x = 2$), so that we did not carry out quantitative measurements. The identification of the x th fraction ($x = 3$ –7) with the x -mer was made by analytical GPC with the monomer and dimer as standards. The weight-average molecular weights M_w of the other test samples were determined by analytical GPC for $M_w < 900$ and from light scattering (LS) measurements in toluene for $M_w > 900$. The details of the LS measurements will be given elsewhere.¹⁴ The ratio of M_w to the number-average molecular weight M_n was also determined by analytical GPC. The values of M_w and M_w/M_n for all the samples used in this work are given in Table I along with those of the weight-average degree of polymerization x_w , where M_w 's of ODMS1 through ODMS7 have been calculated from their chemical formulas.

The solvent cyclohexane used for the determination of $\langle \mu^2 \rangle$ and the solvents benzene and chlorobenzene used for the calibration of a dielectric cell were purified according to standard procedures. The solvent chloroform-*d* used for NMR measurements was of reagent grade.

Dielectric Constant. For a determination of the derivative $(d\epsilon/dw)_0$ with respect to the weight fraction w at $w = 0$, which was required for the evaluation of $\langle \mu^2 \rangle$, the dielectric constant ϵ was measured as a function of w for cyclohexane solutions of the PDMS samples at 25.0 °C in the frequency range from 3 to 100 kHz with a transformer bridge (Ando Electric Co., Tokyo, Type TR-10C) equipped with a function generator (Ando Electric Co., Type WBG-9) and a null-point detector (Ando Electric Co.,

Type BDA-9). The dielectric cell used was a concentric cylindrical one (Ando Electric Co., Type LE-22) whose sample volume and vacuum capacitance were ca. 5 cm³ and ca. 18 pF, respectively. It was contained in a waterproof plastic case, which was immersed in a water bath for thermostating. The temperature in the case was regulated to ± 0.05 °C. The cell was calibrated at 25.0 °C with cyclohexane, benzene, and chlorobenzene as reference liquids. The used values of ϵ at 25.0 °C were 2.015 for cyclohexane,¹⁶ 2.274 for benzene,¹⁶ and 5.607 for chlorobenzene. The value for chlorobenzene was evaluated by interpolation from the literature values 5.670 and 5.372 at 21.0 and 40.0 °C, respectively.¹⁷ The estimated error in capacitance measurements is ± 0.005 pF.

The concentrations of the test solutions were in the range from ca. 2 to ca. 10 wt % for the samples ODMS2 through ODMS4 and from ca. 0.5 to ca. 8 wt % for the samples ODMS5 through PDMS20. For the sample ODMS1 (monomer), the measurements were carried out over the whole range of concentration. For all solutions, the observed ϵ was independent of frequency in the above range.

Refractive Index Increment. The refractive index increment $(dn/dw)_0$ as defined as the derivative of the refractive index n with respect to w at $w = 0$, which was required for the evaluation of $\langle \mu^2 \rangle$, was measured at 436 nm for all the PDMS samples in cyclohexane at 25 °C by the use of a Shimadzu differential refractometer.

Specific Volume. For a determination of the derivative $(dv/dw)_0$ with respect to w at $w = 0$, which was required for the evaluation of $\langle \mu^2 \rangle$, the specific volume v was determined for cyclohexane solutions of all the PDMS samples at 25.0 °C from the density measured with a pycnometer of the Lipkin–Davison type having a volume of 10 cm³. The concentrations of the test solutions were in the range from ca. 0.5 to ca. 7 wt % for the samples ODMS2 through ODMS71 and from ca. 0.1 to ca. 3 wt % for the samples PDMS1 through PDMS20. For the sample ODMS1 (monomer), the difference between the solute and solvent densities was so small that the measurements were carried out over a rather wide concentration range, i.e., from ca. 2 to ca. 50 wt %.

Results

Before presenting experimental results for the dielectric constant, refractive index increment, and specific volume, we first summarize the procedure used for the evaluation of $\langle \mu^2 \rangle$ from them. For a dilute solution of a polar solute dissolved in a nonpolar solvent, the molar polarization P of the solute as defined as the polarizability of the solute molecule multiplied by $4\pi N_A/3$ with N_A Avogadro's number may be related to $\langle \mu^2 \rangle$ of the solute molecule by the Debye equation¹⁸

$$P = \frac{4\pi N_A}{9k_B T} \langle \mu^2 \rangle + P^D \quad (1)$$

where k_B is Boltzmann's constant, T is the absolute temperature, and P^D is the distortional polarization. As usually done, we assume that P^D is composed of the electric polarization P^E and the atomic one P^A as

$$P^D = P^E + P^A \quad (2)$$

Then $\langle \mu^2 \rangle$ may be evaluated from the equation

$$\langle \mu^2 \rangle = \frac{9k_B T}{4\pi N_A} (P - P^E - P^A) \quad (3)$$

We adopt the Halverstadt–Kumler equations¹⁹ for P and P^E

$$P = \frac{\epsilon_0 - 1}{\epsilon_0 + 2} M \left[\left(\frac{dv}{dw} \right)_0 + v_0 \right] + \frac{3Mv_0}{(\epsilon_0 + 2)^2} \left(\frac{d\epsilon}{dw} \right)_0 \quad (4)$$

$$P^E = \frac{n_0^2 - 1}{n_0^2 + 2} M \left[\left(\frac{dv}{dw} \right)_0 + v_0 \right] + \frac{6Mn_0 v_0}{(n_0^2 + 2)^2} \left(\frac{dn}{dw} \right)_0 \quad (5)$$

Table II
Values of $(d\epsilon/dw)_0$, $(dn/dw)_0$, and $(dv/dw)_0$ for Oligo- and Poly(dimethylsiloxane)s in Cyclohexane at 25.0 °C

sample	$(d\epsilon/dw)_0$	$(dn/dw)_0$	$(dv/dw)_0, \text{cm}^3/\text{g}$
ODMS1	0.1822	-0.04582	0.01481
ODMS2	0.2716	-0.03786	-0.08035
ODMS3	0.3347	-0.03372	-0.1151
ODMS4	0.3878	-0.03019	-0.1439
ODMS5	0.4126	-0.02759	-0.1676
ODMS6	0.4362	-0.02647	-0.1788
ODMS7	0.4628	-0.02551	-0.1888
ODMS10	0.4872	-0.02339	-0.2072
ODMS11	0.5117	-0.02211	-0.2191
ODMS14	0.5176	-0.02136	-0.2266
ODMS18	0.5332	-0.02046	-0.2316
ODMS24	0.5359	-0.01979	-0.2452
ODMS35	0.5523	-0.01897	-0.2465
ODMS71	0.5330	-0.01820	-0.2541
PDMS1	0.5435	-0.01750	-0.2579
PDMS2	0.5603	-0.01709	-0.2624
PDMS3	0.5698	-0.01678	-0.2641
PDMS20	0.5763	-0.01724	-0.2634

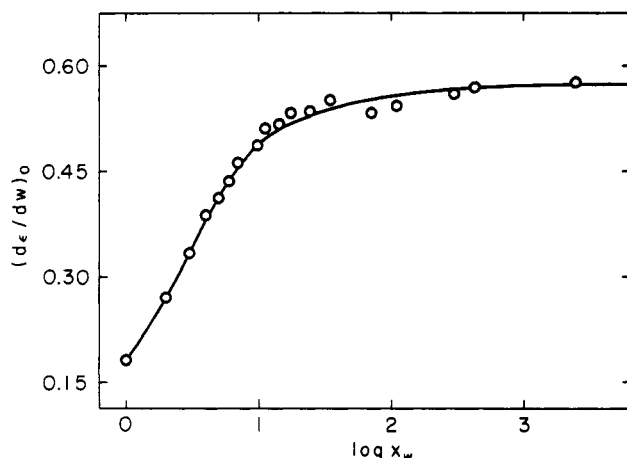


Figure 1. $(d\epsilon/dw)_0$ plotted against the logarithm of x_w for PDMS in cyclohexane at 25.0 °C.

where the subscript 0 indicates the values for the pure solvent (cyclohexane in this case). We note that, in the derivation of eqs 4 and 5, the effect of the internal field has been taken into account by the use of the Clausius-Mosotti equation and that strictly eq 5 has been derived by Riande and Mark²⁰ following the procedure of Halverstadt and Kumler. We also note that, as shown by Matsuo and Stockmayer,²¹ eqs 3–5 are equivalent to the equations derived by Guggenheim²² and Smith.²³ As for P^A , we adopt the values reported by Beevers et al.²⁴ for undiluted PDMS at 25.0 °C, assuming that the difference between the values for undiluted and diluted samples is small. Their results for P^A (in cm^3/mol) for large x_w may well be reproduced by their own relation

$$P^A = -0.962 + 6.48x \quad (6)$$

and we calculate P^A from eq 6 for $x_w \geq 7$. Thus we evaluate $\langle \mu^2 \rangle$ from eqs 3–5 with experimental results for $(d\epsilon/dw)_0$, $(dn/dw)_0$, and $(dv/dw)_0$ together with the above values of P^A .

The values of $(d\epsilon/dw)_0$, $(dn/dw)_0$, and $(dv/dw)_0$ are given in Table II and are plotted against the logarithm of x_w in Figures 1–3, respectively. In all cases, the observed values vary smoothly as functions of x_w , indicating that the measurements were carried out very accurately. Both $(d\epsilon/dw)_0$ and $(dn/dw)_0$ steeply decrease with decreasing x_w for $x_w < 50$, while $(dv/dw)_0$ steeply increases with decreasing x_w in the same range. All these values become constant for $x_w > 100$.

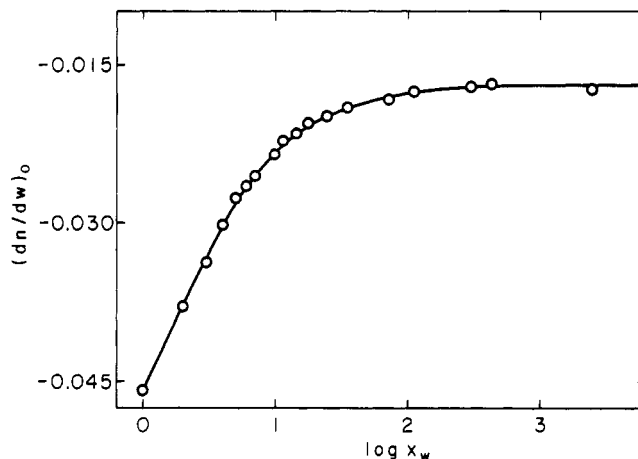


Figure 2. $(dn/dw)_0$ plotted against the logarithm of x_w for PDMS in cyclohexane at 25.0 °C.

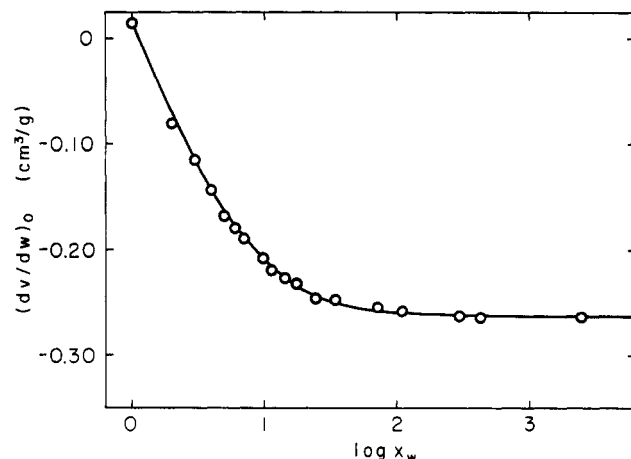


Figure 3. $(dv/dw)_0$ plotted against the logarithm of x_w for PDMS in cyclohexane at 25.0 °C.

The values of P calculated from eq 4 with those of $(d\epsilon/dw)_0$ and $(dv/dw)_0$ given in Table II and the values of P^E from eq 5 with those of $(dn/dw)_0$ and $(dv/dw)_0$ also given in Table II are given in Table III. Here, the values of ϵ_0 , n_0 , and v_0 used for cyclohexane at 25.0 °C are 2.015,¹⁶ 1.4328, and 1.2927 cm^3/g , respectively. In Table III are also given the values of $\langle \mu^2 \rangle$ calculated as mentioned above.

Discussion

Dependence of $\langle \mu^2 \rangle$ on x_w . Figure 4 shows plots of the ratio $\langle \mu^2 \rangle/x_w$ against the logarithm of x_w for PDMS. The unfilled circles represent the present data in cyclohexane at 25.0 °C. For comparison, the data obtained by Riande and Mark²⁰ in cyclohexane at 30.0 °C (unfilled upward triangles) and the data obtained for undiluted PDMS by Sutton and Mark¹¹ at 20.0 or 25.0 °C (filled upward triangles), by Liao and Mark¹² at 25.0 °C (filled downward triangles), and by Beevers et al.²⁴ at 25.0 °C (filled squares) are also shown in the figure. The present results show that, as x_w is increased, $\langle \mu^2 \rangle/x_w$ first increases very steeply for $x_w \leq 4$, then passes through a maximum, and finally approaches promptly its asymptotic value, which is substantially constant for $x_w \geq 20$.

The values of $\langle \mu^2 \rangle/x_w$ by Riande and Mark,²⁰ which were obtained under almost the same condition as ours, are appreciably smaller than our values and its dependence on x_w is also different. However, such a direct comparison requires a remark. Although our procedure for the determination of $\langle \mu^2 \rangle$ from the experimental data for $(d\epsilon/dw)_0$, $(dn/dw)_0$, and $(dv/dw)_0$ is the same as theirs,

Table III
Values of P , P^E , and $\langle \mu^2 \rangle$ for Oligo- and Poly(dimethylsiloxane)s in Cyclohexane at 25.0 °C

sample	P , cm ³ /mol	P^E , cm ³ /mol	$\langle \mu^2 \rangle$, D ²
ODMS1	60.75	50.12	0.05839
ODMS2	87.91	68.45	0.2679
ODMS3	117.5	87.99	0.5059
ODMS4	147.7	107.7	0.8587
ODMS5	176.1	125.6	1.045
ODMS6	206.1	144.8	1.202
ODMS7	237.1	163.8	1.418
ODMS10	319.2	217.0	1.946
ODMS11	364.4	243.9	2.367
ODMS14	448.9	299.2	2.878
ODMS18	551.0	364.0	3.660
ODMS24	747.7	491.5	4.858
ODMS35	1060	681.1	7.576
ODMS71	2098	1383	12.49
PDMS1	3240	2123	19.88
PDMS2	8715	5642	56.38
PDMS3	12660	8162	84.50
PDMS20	72960	46800	498.4

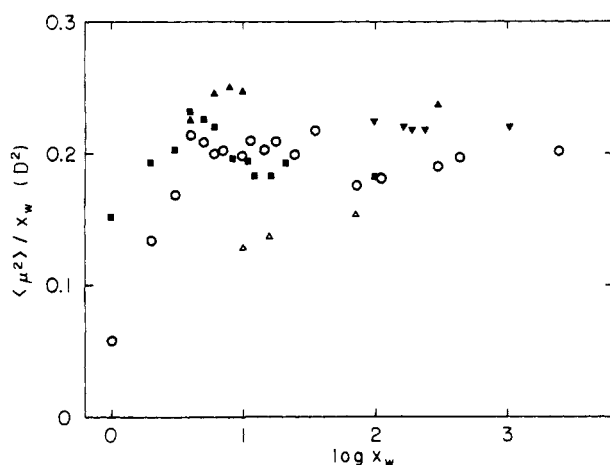


Figure 4. Plots of $\langle \mu^2 \rangle / x_w$ against the logarithm of x_w for PDMS: (O) present data in cyclohexane at 25.0 °C; (Δ) data in cyclohexane at 30.0 °C by Riande and Mark;²⁰ (▲) data in the undiluted state at 20.0 and 25.0 °C by Sutton and Mark;¹¹ (▼) data in the undiluted state at 25.0 °C by Liao and Mark;¹² (■) data in the undiluted state at 25.0 °C by Beevers et al.²⁴

our values of P^A are different from their values which were evaluated from the relation $P^A = 2.15 + 5.66x$ cm³/mol derived by Sutton and Mark¹¹ on the basis of the experimental data obtained by Dasgupta and Smyth.²⁵ For comparison, therefore, we have evaluated $\langle \mu^2 \rangle$ from eqs 3–6 with their experimental data for $(d\epsilon/dw)_0$, $(dn/dw)_0$, and $(dv/dw)_0$ for the three samples. The obtained values of $\langle \mu^2 \rangle / x_w$ become almost independent of x_w , but their mean is only 0.120 D², which is still appreciably (ca. 40%) smaller than ours. This difference in $\langle \mu^2 \rangle / x_w$ does not arise from that in P^A but from those in $(d\epsilon/dw)_0$, $(dn/dw)_0$, and $(dv/dw)_0$.

The values of $\langle \mu^2 \rangle / x_w$ obtained by Sutton and Mark¹¹ and by Liao and Mark¹² for undiluted PDMS, which have been used in the previous preliminary analysis,¹³ are ca. 20% larger than ours for $x_w \geq 7$ but exhibit qualitatively the same behavior as ours; i.e., $\langle \mu^2 \rangle / x_w$ as a function of x_w has a maximum. We note that their values of $\langle \mu^2 \rangle$ were calculated from the Onsager equation with the observed values of ϵ together with the values of P^A obtained from the above relation given by Sutton and Mark.¹¹ Thus the difference seems to arise partly from that in the procedure of evaluating $\langle \mu^2 \rangle$. On the other hand, our results are unexpectedly in good agreement with those obtained by Beevers et al.²⁴ for undiluted PDMS for $x_w \geq 4$, although

our values are appreciably smaller than theirs for $x_w \leq 3$. This agreement seems rather natural, considering the facts that they determined $\langle \mu^2 \rangle$ from the Clausius–Mosotti equation and that we have used their values of P^A . The disagreement for very small x_w may be regarded as arising from the fact that the difference between the diluted and undiluted states in the internal field becomes large for small x_w .

Now, before proceeding to make an analysis of the data on the basis of the HW chain, we consider the excluded-volume effect on $\langle \mu^2 \rangle$ for PDMS. On both experimental²⁶ and theoretical^{27,28} sides, no excluded-volume effect on $\langle \mu^2 \rangle$ has been considered to exist in polymer chains having type-B dipoles. Recently, however, Mattice and Carpenter²⁹ have claimed on the basis of Monte Carlo calculations that the effect exists even in such polymer chains, and Mansfield³⁰ has shown a possibility of the effect on $\langle \mu^2 \rangle$ due to the non-Gaussian nature of the chain. We note that the expansion factor for $\langle \mu^2 \rangle$ for such chains does not depend on x for very large x ,³⁰ its dependence on x being different from those for $\langle S^2 \rangle$ or $[\eta]$. At the present time, therefore, we cannot verify theoretically that there is no excluded-volume effect on $\langle \mu^2 \rangle$ for PDMS.

On the other hand, according to the Yamakawa–Stockmayer–Shimada theory^{31–33} of the excluded-volume effect on $\langle S^2 \rangle$ for the KP and HW chains, the effect may be considered to appear for the chain of a contour length more than 3 times as long as the static stiffness parameter λ^{-1} . This bound corresponds to $x \approx 20$ for the case of PDMS, which has been estimated from the HW model parameters determined from the previous preliminary analysis.¹³ As mentioned above, the present values of $\langle \mu^2 \rangle / x_w$ have already attained its asymptotic value for $x_w > 20$. Therefore, it turns out that the excluded-volume effect on $\langle \mu^2 \rangle$ for PDMS in cyclohexane is negligibly small if any. This conclusion may also be supported by the fact that the present data are in good agreement with those obtained by Beevers et al.²⁴ for undiluted PDMS, for which there is no excluded-volume effect. Thus, in the next subsection, we analyze the present data, regarding them as the results for unperturbed chains.

HW Model Parameters. For the HW chain of contour length L (without excluded volume), whose equilibrium conformational behavior is described by the constant differential geometrical curvature κ_0 and torsion τ_0 of the characteristic helix taken at the minimum of energy and the above-mentioned static stiffness parameter λ^{-1} as defined as the bending force constant divided by $k_B T/2$, $\langle \mu^2 \rangle$ may be written in the form¹³

$$\langle \mu^2 \rangle = (\lambda^{-1} m)^2 f_R(\lambda L; \lambda^{-1} \hat{\kappa}_0, \lambda^{-1} \hat{\tau}_0) \quad (7)$$

with m the magnitude of the local electric dipole moment vector \mathbf{m} per unit contour length. The function $f_R(\lambda L; \lambda^{-1} \hat{\kappa}_0, \lambda^{-1} \hat{\tau}_0)$ is defined from the mean-square end-to-end distance $\langle R^2 \rangle$ of the HW chain of contour length L as

$$\langle R^2 \rangle = \lambda^{-2} f_R(\lambda L; \lambda^{-1} \hat{\kappa}_0, \lambda^{-1} \hat{\tau}_0) \quad (8)$$

and $\hat{\kappa}_0$ and $\hat{\tau}_0$ are defined by

$$\hat{\kappa}_0 = (\lambda^2 \nu^2 - \hat{\tau}_0^2)^{1/2} \quad (9)$$

$$\hat{\tau}_0 = (\kappa_0 m_\eta + \tau_0 m_\zeta) / m \quad (10)$$

where ν is given by

$$\nu = (\lambda^{-2} \kappa_0^2 + \lambda^{-2} \tau_0^2)^{1/2} = (\lambda^{-2} \hat{\kappa}_0^2 + \lambda^{-2} \hat{\tau}_0^2)^{1/2} \quad (11)$$

and m_η and m_ζ are the η and ζ components of \mathbf{m} expressed

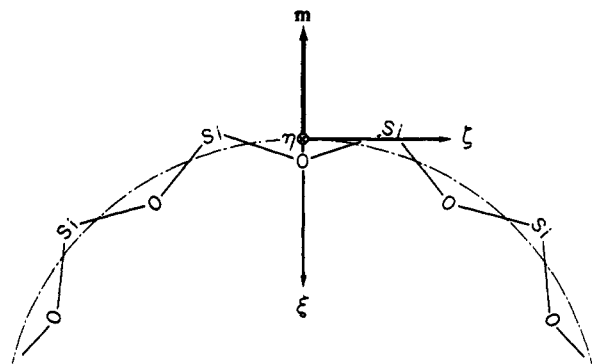


Figure 5. Local electric dipole moment vector \mathbf{m} (see the text). in the localized Cartesian coordinate system, respectively. The function f_R is explicitly given by³⁴

$$f_R(\lambda L; \lambda^{-1}\kappa_0, \lambda^{-1}\tau_0) = \lambda L - \frac{1}{2} + \frac{1}{2}e^{-2\lambda L} + \frac{\lambda^{-2}\kappa_0^2}{4 + \nu^2} \left[-\lambda L + \frac{12 + \nu^2}{2(4 + \nu^2)} + e^{-\lambda L} \left\{ \frac{2}{(4 + \nu^2)\nu^2} [(4 - \nu^2) \cos(\nu\lambda L) - 4\nu \sin(\nu\lambda L)] - \frac{4 + \nu^2}{2\nu^2} \right\} \right] \quad (12)$$

If we introduce the function f_μ defined by

$$f_\mu(\lambda L; \lambda^{-1}\kappa_0, \lambda^{-1}\tau_0, \lambda^{-1}\mathbf{m}) \equiv f_R(\lambda L; \lambda^{-1}\kappa_0, \lambda^{-1}\tau_0) \quad (13)$$

then $\langle \mu^2 \rangle/x$ and x are related to $f_\mu(\lambda L)$ and L as

$$\langle \mu^2 \rangle/x = (\lambda^{-1}m)^2 (\lambda^{-1}M_L/M_0)^{-1} [f_\mu(\lambda L; \lambda^{-1}\kappa_0, \lambda^{-1}\tau_0, \lambda^{-1}\mathbf{m})/\lambda L] \quad (14)$$

and

$$\log x = \log(\lambda L) + \log(\lambda^{-1}M_L/M_0) \quad (15)$$

respectively, where M_L is the shift factor as defined as the molecular weight per unit contour length and M_0 is the molecular weight per repeat unit. From eqs 12–14, the asymptotic value of $\langle \mu^2 \rangle/x_w$ is seen to be equal to $\lambda^{-1}M_0m^2/M_L$. Thus the quantities $\lambda^{-1}M_L$ and $\lambda^{-1}m$ may be determined from a best fit of a plot of the theoretical $\langle \mu^2 \rangle/x$ against $\log(\lambda L)$ for properly chosen values of $\lambda^{-1}\kappa_0$, $\lambda^{-1}\tau_0$, and \mathbf{m} to that of the observed $\langle \mu^2 \rangle/x_w$ against $\log x_w$.

As mentioned in the Introduction, the procedure of assigning the localized Cartesian coordinate system (ξ , η , ζ) affixed to the HW chain to the repeat unit (Si–O–Si) of the PDMS chain has been established in previous studies,^{13,35} as depicted in Figure 5. That is, the ζ axis is taken along a line passing through the two successive Si atoms, the ξ axis is in the plane of the Si–O and O–Si bonds with its positive direction chosen at an acute angle with the Si→O bond, and the η axis completes the right-handed system. (Although this system is not the same as that used in ref 13, the two systems have been shown to be equivalent to each other as far as $\langle \mu^2 \rangle$ is concerned.³⁴) Then the vector \mathbf{m} is in the negative direction of the ξ axis, since the permanent dipole moment of PDMS arises from the O–Si bonds. Thus the components of \mathbf{m} expressed in this localized coordinate system may be set equal to $(-m, 0, 0)$. As seen from eqs 9 and 10, the two parameters κ_0 and τ_0 cannot be determined independently in this case of $m_\eta = m_\zeta = 0$. Thus we further set $\tau_0 = 0$ as before.¹³ This assumption seems rather reasonable, considering the symmetry properties of the (symmetric) PDMS chain.³⁵

Figure 6 shows plots of $\langle \mu^2 \rangle/x_w$ against the logarithm of x_w for PDMS in cyclohexane at 25.0 °C. The unfilled

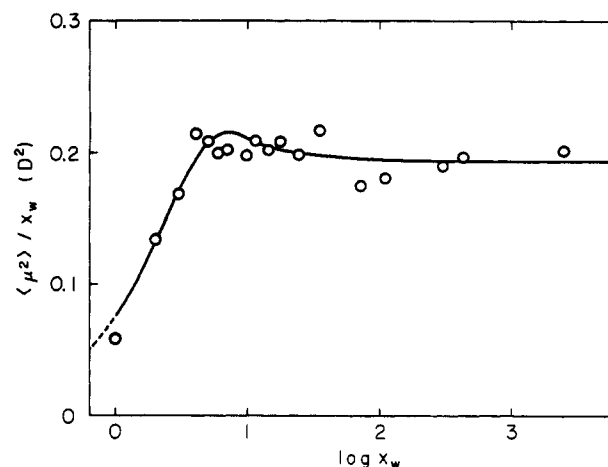


Figure 6. Comparison between the present observed and theoretical values of $\langle \mu^2 \rangle/x_w$ for PDMS in cyclohexane at 25.0 °C. The solid curve represents the best fit HW theoretical values (see the text).

circles represent the present experimental values, and the solid curve represents the best fit theoretical values calculated from eq 13 with $\lambda^{-1}\kappa_0 = 2.6$, $\lambda^{-1}\tau_0 = 0$, $\lambda^{-1}M_L = 450$, and $\lambda^{-1}m = 1.78$ D. It is seen that the theory may well explain the dependence of $\langle \mu^2 \rangle/x_w$ on x_w , especially its maximum. It should be noted that the value 2.6 of $\lambda^{-1}\kappa_0$ coincides with the one determined in the previous preliminary analysis.¹³ Finally, we note that the asymptotic value 0.17 D² of $\langle \mu^2 \rangle/x$ (in the limit of $x \rightarrow \infty$) evaluated by Mark³⁶ on the basis of the rotational isomeric state model is appreciably smaller than the present experimental values.

Dipole Moment per Repeat Unit. The permanent electric dipole moment m_0 per repeat unit of the PDMS chain is evaluated to be 0.29 D from the relation $m_0 = M_0m/M_L$ with the values of $\lambda^{-1}M_L$ and $\lambda^{-1}m$ determined in the preceding subsection. It is ca. 10% smaller than the value 0.33 D obtained in the previous analysis¹³ of the data obtained by Sutton and Mark¹¹ and by Liao and Mark¹² for undiluted PDMS. This difference arises mainly from the difference between the present and their data in $\langle \mu^2 \rangle/x_w$ for large x_w . The present value 0.29 D of m_0 is also smaller than the value 0.38 D evaluated from the value 0.14 D² of $\langle \mu^2 \rangle$ obtained by Dasgupta et al.³⁷ for the PDMS monomer in the undiluted state but is rather in better agreement with the value 0.24 D evaluated from the present value 0.058 D² of $\langle \mu^2 \rangle$ for the monomer.

Concluding Remarks

We have been able to determine the two sets of the HW model parameters, $\lambda^{-1}\kappa_0$ and $\lambda^{-1}M_L$, for PDMS from the analysis of its $\langle \mu^2 \rangle$ in cyclohexane at 25.0 °C, assuming $\lambda^{-1}\tau_0 = 0$. The value 2.6 of $\lambda^{-1}\kappa_0$ coincides with the one determined in the previous analysis of $\langle \mu^2 \rangle$ for undiluted PDMS, indicating that the PDMS chain has rather strong helical nature also in dilute solution, as expected from its chemical structure. (The term “strong helical nature” means that the chain contour retains large helical portions even with thermal fluctuations. Quantitatively, such a chain has $\lambda^{-1}\kappa_0 \gtrsim 2$ and $\lambda^{-1}\tau_0 \lesssim \lambda^{-1}\kappa_0/\pi$.³⁸) Unfortunately, however, all the HW model parameters cannot be determined separately from $\langle \mu^2 \rangle$ alone since it is not a quantity that is directly related to the chain dimension. The complete determination of them requires other dilute-solution properties relating to the chain dimension. Thus we will make an experimental study of transport coefficients in the forthcoming paper,¹⁴ in which the values of

$\lambda^{-1}\kappa_0$ and $\lambda^{-1}\tau_0$ are assumed to be identical with the ones determined in the present study.

Acknowledgment. This research was supported in part by a Grant-in-Aid (0143 0018) from the Ministry of Education, Science, and Culture, Japan.

References and Notes

- (1) Yamakawa, H. *Annu. Rev. Phys. Chem.* **1984**, *35*, 23.
- (2) Yamakawa, H. In *Molecular Conformation and Dynamics of Macromolecules in Condensed Systems*; Nagasawa, M., Ed.; Elsevier: Amsterdam, The Netherlands, 1988; p 21.
- (3) Konishi, T.; Yoshizaki, T.; Shimada, J.; Yamakawa, H. *Macromolecules* **1989**, *22*, 1921.
- (4) Einaga, Y.; Koyama, H.; Konishi, T.; Yamakawa, H. *Macromolecules* **1989**, *22*, 3149.
- (5) Konishi, T.; Yoshizaki, T.; Saito, T.; Einaga, Y.; Yamakawa, H. *Macromolecules* **1990**, *23*, 290.
- (6) Yamada, T.; Yoshizaki, T.; Yamakawa, H. *Macromolecules*, in press.
- (7) Tamai, Y.; Konishi, T.; Einaga, Y.; Fujii, M.; Yamakawa, H. *Macromolecules* **1990**, *23*, 4067.
- (8) Fujii, Y.; Tamai, Y.; Konishi, T.; Yamakawa, H. *Macromolecules* **1991**, *24*, 1608.
- (9) Abe, F.; Einaga, Y.; Yamakawa, H. *Macromolecules* **1991**, *24*, 4423.
- (10) Kratky, O.; Porod, G. *Recl. Trav. Chim.* **1949**, *68*, 1106.
- (11) Sutton, C.; Mark, J. E. *J. Chem. Phys.* **1971**, *54*, 5011.
- (12) Liao, S. C.; Mark, J. E. *J. Chem. Phys.* **1973**, *59*, 3825.
- (13) Yamakawa, H.; Shimada, J.; Nagasaka, K. *J. Chem. Phys.* **1979**, *71*, 3573.
- (14) Yamada, T.; Koyama, H.; Yoshizaki, T.; Einaga, Y.; Yamakawa, H.; to be submitted to *Macromolecules*.
- (15) Stockmayer, W. H. *Pure Appl. Chem.* **1967**, *15*, 539.
- (16) Maryott, A. A.; Smith, E. R. Table of Dielectric Constants of Pure Liquids; NBS Circular 514; 1951.
- (17) Le Fevre, R. J. W. *Trans. Faraday Soc.* **1938**, *34*, 1127.
- (18) Debye, P. *Polar Molecules*; Chemical Catalog: New York, 1929.
- (19) Halverstadt, L. F.; Kumler, W. D. *J. Am. Chem. Soc.* **1942**, *64*, 2988.
- (20) Riande, E.; Mark, J. E. *Eur. Polym. J.* **1984**, *20*, 517.
- (21) Matsuo, K.; Stockmayer, W. H. *J. Phys. Chem.* **1981**, *85*, 3307.
- (22) Guggenheim, E. A. *Trans. Faraday Soc.* **1949**, *45*, 714.
- (23) Smith, J. W. *Electric Dipole Moments*; Butterworths: London, 1955; p 47.
- (24) Beevers, M. S.; Mumby, S. J.; Clarson, S. J.; Semlyen, J. A. *Polymer* **1983**, *24*, 1565.
- (25) Dasgupta, S.; Smyth, C. P. *J. Chem. Soc.* **1967**, *47*, 2911.
- (26) Marchal, J.; Benoit, H. *J. Polym. Sci.* **1957**, *23*, 223.
- (27) Nagai, K.; Ishikawa, T. *Polym. J.* **1971**, *2*, 416.
- (28) Doi, M. *Polym. J.* **1972**, *3*, 252.
- (29) Mattice, W. L.; Carpenter, D. K. *Macromolecules* **1984**, *17*, 625.
- (30) Mansfield, M. L. *Macromolecules* **1986**, *19*, 1427.
- (31) Yamakawa, H.; Stockmayer, W. H. *J. Chem. Phys.* **1972**, *57*, 2843.
- (32) Yamakawa, H.; Shimada, J. *J. Chem. Phys.* **1985**, *83*, 2067.
- (33) Shimada, J.; Yamakawa, H. *J. Chem. Phys.* **1986**, *85*, 591.
- (34) Yamakawa, H.; Fujii, M. *J. Chem. Phys.* **1976**, *64*, 5222.
- (35) Yamakawa, H.; Shimada, J. *J. Chem. Phys.* **1979**, *70*, 609.
- (36) Mark, J. E. *J. Chem. Phys.* **1968**, *49*, 1398.
- (37) Dasgupta, S.; Garg, S. K.; Smyth, C. P. *J. Am. Chem. Soc.* **1967**, *89*, 2243.
- (38) Yamakawa, H.; Shimada, J.; Fujii, M. *J. Chem. Phys.* **1978**, *68*, 2140.

Registry No. $\text{CH}_3\text{Si}(\text{CH}_3)_2\text{OSi}(\text{CH}_3)_3$, 107-46-0; $\text{CH}_3[\text{Si}(\text{CH}_3)_2\text{O}]_2\text{Si}(\text{CH}_3)_3$, 107-51-7; $\text{CH}_3[\text{Si}(\text{CH}_3)_2\text{O}]_3\text{Si}(\text{CH}_3)_3$, 141-62-8; $\text{CH}_3[\text{Si}(\text{CH}_3)_2\text{O}]_4\text{Si}(\text{CH}_3)_3$, 141-63-9; $\text{CH}_3[\text{Si}(\text{CH}_3)_2\text{O}]_5\text{Si}(\text{CH}_3)_3$, 107-52-8; $\text{CH}_3[\text{Si}(\text{CH}_3)_2\text{O}]_6\text{Si}(\text{CH}_3)_3$, 541-01-5; $\text{CH}_3[\text{Si}(\text{CH}_3)_2\text{O}]_7\text{Si}(\text{CH}_3)_3$, 556-69-4.